The Protein Composition of Mitotic Chromosomes Determined Using Multiclassifier Combinatorial Proteomics

Cell

Resource

The Protein Composition of Mitotic Chromosomes Determined Using Multiclassifier Combinatorial Proteomics

Shinya Ohta,[1,6] Jimi-Carlo Bukowski-Wills,[1,2,6] Luis Sanchez-Pulido,[4] Flavia de Lima Alves,[1] Laura Wood,[1] Zhuo A. Chen,[1] Melpi Platani,[1] Lutz Fischer,[1] Damien F. Hudson,[1,5] Chris P. Ponting,[4] Tatsuo Fukagawa,[3] William C. Earnshaw,[1,*] and Juri Rappsilber[1,*]

[1]Wellcome Trust Centre for Cell Biology

[2]Centre for Systems Biology at Edinburgh, School of Biological Sciences
University of Edinburgh, Edinburgh EH9 3JR, UK

[3]Department of Molecular Genetics, National Institute of Genetics and The Graduate University for Advanced Studies, Mishima, Shizuoka 411-8540, Japan

[4]MRC Functional Genomics Unit, Department of Physiology, Anatomy and Genetics, University of Oxford, Oxford OX1 3QX, UK

[5]Present address: Murdoch Children's Research Institute, Royal Children's Hospital, Melbourne, Victoria 3052, Australia

[6]These authors contributed equally to this work

*Correspondence: bill.earnshaw@ed.ac.uk (W.C.E.), juri.rappsilber@ed.ac.uk (J.R.)

DOI 10.1016/j.cell.2010.07.047

SUMMARY

Despite many decades of study, mitotic chromosome structure and composition remain poorly characterized. Here, we have integrated quantitative proteomics with bioinformatic analysis to generate a series of independent classifiers that describe the ~4,000 proteins identified in isolated mitotic chromosomes. Integrating these classifiers by machine learning uncovers functional relationships between protein complexes in the context of intact chromosomes and reveals which of the ~560 uncharacterized proteins identified here merits further study. Indeed, of 34 GFP-tagged predicted chromosomal proteins, 30 were chromosomal, including 13 with centromere-association. Of 16 GFP-tagged predicted nonchromosomal proteins, 14 were confirmed to be nonchromosomal. An unbiased analysis of the whole chromosome proteome from genetic knockouts of kinetochore protein *Ska3/Rama1* revealed that the APC/C and RanBP2/RanGAP1 complexes depend on the Ska complex for stable association with chromosomes. Our integrated analysis predicts that up to 97 new centromere-associated proteins remain to be discovered in our data set.

INTRODUCTION

As cells enter mitosis, chromosomes undergo a remarkable series of physiological and structural transformations known as chromosome condensation. This process involves individualization of the chromosomal territories to create the characteristic mitotic chromosome morphology and maturation of the kinetochores so that chromosomes can align and segregate on the mitotic spindle. Our understanding of the mechanisms underlying chromosome condensation is still fragmentary. These processes can be fully understood only when all components of mitotic chromosomes have been identified and functional relationships between them determined. We have developed a new approach that we term multiclassifier combinatorial proteomics (MCCP) to do this.

The current list of mitotic chromatin proteins reported in proteomic studies is surprisingly short. Early analyses described 62 and 79 proteins, respectively, in mitotic chromosome scaffolds (Morrison et al., 2002; Gassmann et al., 2005). A later study identified > 250 proteins that bound to sperm chromatin in *Xenopus* egg extracts in vitro, revealing the kinetochore protein Bod1 (Porter et al., 2007). Other studies identified ~240 proteins, subsequently corrected to roughly 50 bona fide putative structural proteins (Uchiyama et al., 2005; Takata et al., 2007). In a targeted study, 98 proteins were identified as shared in isolated telomeres from wild-type and ALT cells (Dejardin and Kingston, 2009). Despite these efforts, currently available proteomics reports miss a significant fraction of known mitotic chromosomal proteins, particularly kinetochore components.

Biochemical analysis of important chromosome substructures such as kinetochores is extremely challenging. The kinetochore is one of the most complex cellular substructures (Cheeseman and Desai, 2008), with over 120 constituents described by a range of approaches (Earnshaw and Rothfield, 1985), including targeted proteomic studies (Obuse et al., 2004; Foltz et al., 2006; Okada et al., 2006; Hori et al., 2008; Amano et al., 2009). Biochemical dissection of kinetochores is complicated by the fact that it is not known to what extent the constituent protein complexes can be recovered in soluble form from chromosomes with their relevant intermolecular associations intact. As described here, those problems can be circumvented by purifying and analyzing whole mitotic chromosomes.

Purifying large cellular structures or organelles free of contaminants is virtually impossible. Genuine components have been distinguished from contaminants in such preparations by subtractive (Schirmer et al., 2003) or quantitative (Foster et al., 2003) proteomics by determining the difference between two near-identical fractions, one enriched and the other depleted of the target structure. In protein correlation profiling, a set of known components was used to define a common intensity profile across neighboring biochemical fractions from sucrose gradients during purification of organelles and this was used to select other proteins that show a similar profile (Andersen et al., 2003). These methods do not recognize cellular background proteins that adhere to the structure of interest due to nonspecific hydrophobic or electrostatic interactions. This type of contamination is particularly relevant for vertebrate mitotic chromosomes.

In the present study, we identified approximately 4000 polypeptides in highly purified chromosomes. We developed a statistical approach for analysis of proteomic data to confirm which known and uncharacterized proteins from this long list are chromosomal. An experimental test of our method led to the identification of 32 chromosomal proteins, including 13 kinetochore-associated proteins. Key to our analysis is the innovative use of *s*table *i*sotope *l*abeling with *a*mino acids in cell *c*ulture (SILAC) (Ong et al., 2002), plus development of a framework to integrate data from multiple classifiers, including nonproteomic classifiers, to reveal proteins of interest and determine functional relationships between protein complexes in the context of whole chromosomes.

RESULTS

Identification of the Proteome of Isolated Mitotic Chromosomes

We isolated mitotic chromosomes from chicken DT40 cells by a refinement of the polyamine method (Lewis and Laemmli, 1982) (Figures 1A and 1B). These preparations are negative for porin in immunoblots (Figure 1C), indicating that mitochondrial contamination (common in chromosome preparations) is low.

Proteomic analysis (Cox and Mann, 2008; de Godoy et al., 2008) of 250 μg of total chromosomal protein identified 4029 proteins in 28 functional categories (Figure 1D and Table S1 available online), including essentially all previously described chromosomal proteins.

When vertebrate cells enter mitosis, the nuclear envelope breaks down and chromosomes are newly exposed to cytoplasmic proteins, organelles and cellular membranes. Since highly positively charged histones contribute ~38% of the chromosome mass and an equivalent amount is highly negatively charged DNA, many charged nonchromosomal proteins exhibit strong adventitious binding to chromosomes. These "hitchhikers" differ from conventional contaminants (e.g., mitochondria), as they are physically associated with the chromosomes before cell lysis and apparently cannot be separated by conventional purification protocols. Thus, the 1331 cytoskeletal, cytoplasmic, mitochondrial, membrane and receptor proteins found in our preparations, may be physically associated with chromosomes following nuclear envelope disassembly, but many not be functionally relevant.

A Classifier Approach to Identify Genuine Mitotic Chromosome Proteins

The presence of hitchhiker proteins complicates the definition of what constitutes a "true" chromosomal protein, as well as the design of biochemical control experiments. For example, comparing mitotic to interphase chromatin is of limited use, since the latter is shielded from the cytoplasm by the nuclear envelope. In such a comparison, cytoplasmic hitchhiker proteins would be scored as mitosis-specific chromosomal proteins.

Here, we describe an approach to study the complex chromosomal proteome that both identifies proteins that merit further study and reveals functional relationships between all chromosomal proteins. We quantify the chromosomal association of each protein in a series of quantitative proteomics experiments, mostly using SILAC technology (Ong et al., 2002). Each experiment provides an independent measure of a protein's association with mitotic chromosomes, which we term a "classifier." Integration of the data obtained with all classifiers enables us to detect patterns in the behavior of groups of proteins that reveal shared membership in protein complexes as well as functional dependency relationships.

The experimental protocols that define the five proteomic classifiers are shown in Figure 1E and all classifiers are summarized below.

Classifier I: Abundance estimation

To estimate the amounts of individual proteins in mitotic chromosomes, we used an established protocol (Rappsilber et al., 2002; Ishihama et al., 2005, 2008) to calculate a scaled protein abundance index based on the number of peptides observed and the number of times that each peptide is observed (spectral count) for each protein. This calculation and its validation are discussed in Extended Experimental Procedures.

In the conventional pie chart of Figure 1D, all proteins are weighted equally, independent of their actual abundance in isolated chromosomes. A more informative representation of chromosome composition is obtained by normalizing each class by its mass, obtained by multiplying the estimated abundance by the predicted molecular mass of each protein (Figure 1F). As expected, histones comprise the bulk of mitotic chromosomal protein (48%). Overall 68% of the protein mass is annotated as chromosomal.

Classifier II: Enrichment in Chromosomes

We expected core chromosomal components like histones or structural proteins would be more abundant in isolated chromosomes than in cytoplasmic extracts. The reverse would be true of background proteins. We therefore mixed isolated chromosomes from mitotic DT40 cells grown in light medium with an equal mass of protein from post-chromosomal extracts of parallel cultures grown with heavy SILAC medium (Figure 1E). Classifier II was calculated as the ratio of light/heavy peaks for each protein. Among the 20% most enriched proteins, chromosomal proteins outnumbered nonchromosomal proteins by 3 to 1. Conversely, among the 20% least enriched proteins, background proteins outnumbered chromosomal proteins 6 to 1.

Classifier III: In Vitro Exchange on Chromosomes

We ranked proteins based on their ability to stably bind to chromosomes during an incubation in cytosol. A crude light chromosome fraction obtained by gentle centrifugation was mixed with

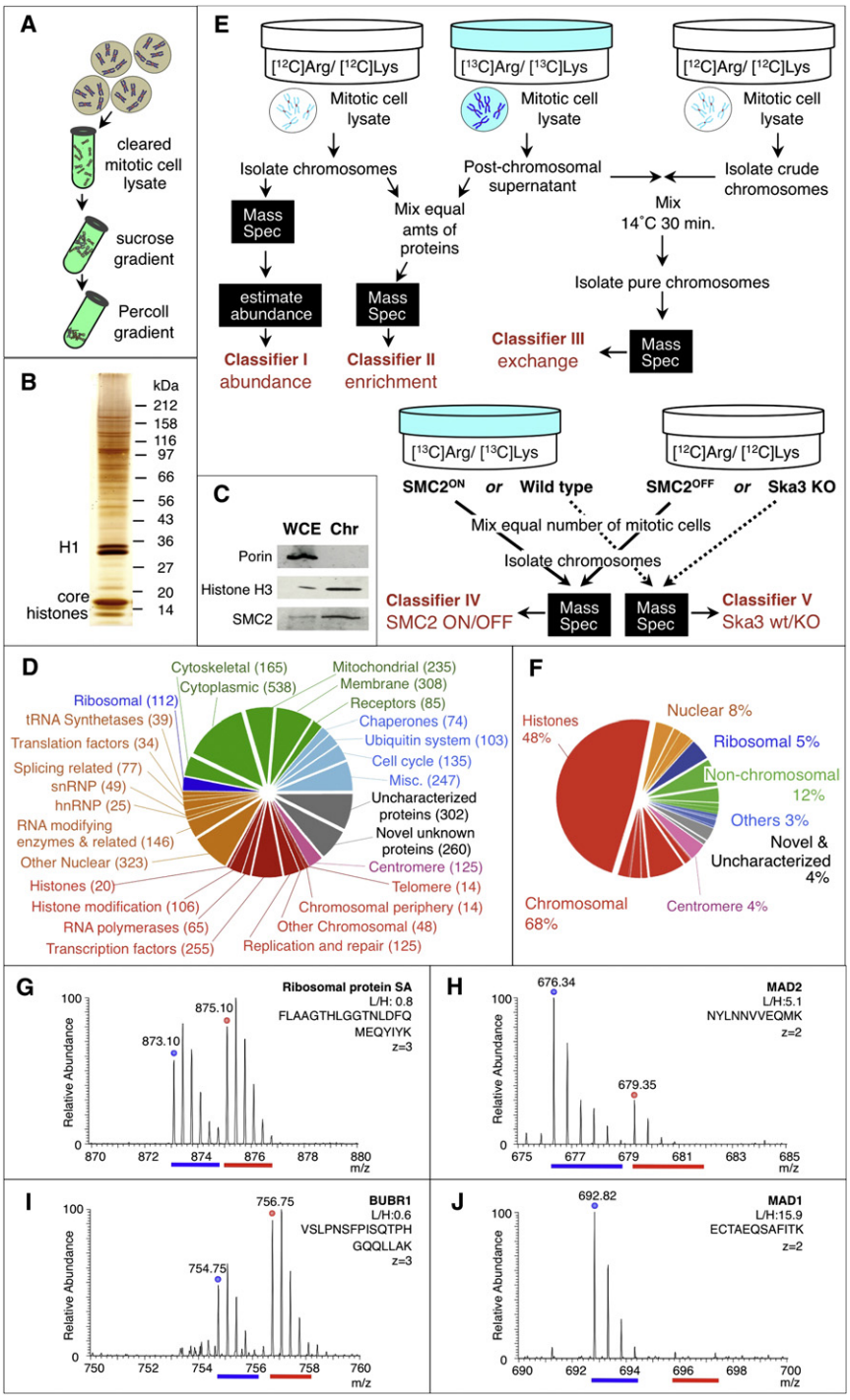

Figure 1. Proteomic Analysis of Mitotic Chromosome Proteins

(A) Outline of chromosome isolation procedure.

(B) Silver-stained gel of isolated chromosomes.

(C) Immunoblot with markers for mitochondria (porin) and chromosomes.

(D) The 28 classes of proteins found in chromosomes.

(E) Experimental designs to prepare samples for determination of classifiers I (abundance), II (enrichment in chromosomes versus post-chromosomal extract), III (exchange onto chromosomes from post-chromosomal cytosol), IV (dependency on SMC2/condensin) and V (dependency on Ska3/RAMA1).

(F–J) (F) Estimated percentages of total chromosomal protein mass in the major classes of proteins. Sample spectra used to calculate classifier III (exchange) values for (G) Ribosomal protein SA (a hitchhiker protein), (H) MAD2, (I) BUBR1 and (J) MAD1. Spectra are plotted as the peak intensity (a measure of abundance) against the mass divided by charge. Peaks of light peptides from chromosomes are indicated by blue bars and heavy peptides bound from cell extracts during the incubation are indicated by red bars. See also Figure S1.

an excess of heavy post-chromosomal extract and incubated to allow proteins to exchange at 14°C for 30 min (Figure 1E). The chromosomes were then subjected to rigorous purification. All heavy proteins identified must have bound to the chromosomes during the incubation in vitro. Classifier III is the light/heavy ratio for each protein identified in this experiment.

The most stable chromosomal-associated proteins were histones (average classifier III = 63), topoisomerase IIα (classifier III = 61) and condensin I (average classifier III = 59). Interestingly, condensin II was more exchangeable (average classifier III = 14). In contrast, the ratios for ~75% of ribosomal proteins were in the range from 0.45 to 3.0 (Figure 1G), indicating significant binding to chromosomes from cytosol during the incubation.

Although we sought to optimize purity rather than preserve functionality of chromosomes, the exchange experiment revealed that at least one aspect of kinetochore function was retained in purified chromosomes. Similar to one recent study (Kulukian et al., 2009), kinetochores of the purified chromosomes can recruit spindle checkpoint proteins Mad2, Bub3, and BubR1 from cytosol (Figures 1H and 1I) but not Mad1 (Figure 1J).

Classifier IV: SMC2 Dependency

We used a conditional genetic knockout of SMC2 in DT40 SMC2$^{ON/OFF}$ cells (Hudson et al., 2003) to compare the composition of mitotic chromosomes formed in the presence or absence of condensin, which is required for structural integrity of mitotic chromosomes. DT40 SMC2^{ON} cells were cultured in SILAC^{heavy} medium. To obtain chromosomes depleted of condensin, cells grown in SILAC^{light} medium were cultured with doxycycline for 30 hr to shut down SMC2 expression prior to the nocodazole block (SMC2^{OFF}). Equal numbers of mitotic cells from the two different populations were mixed and mitotic chromosomes

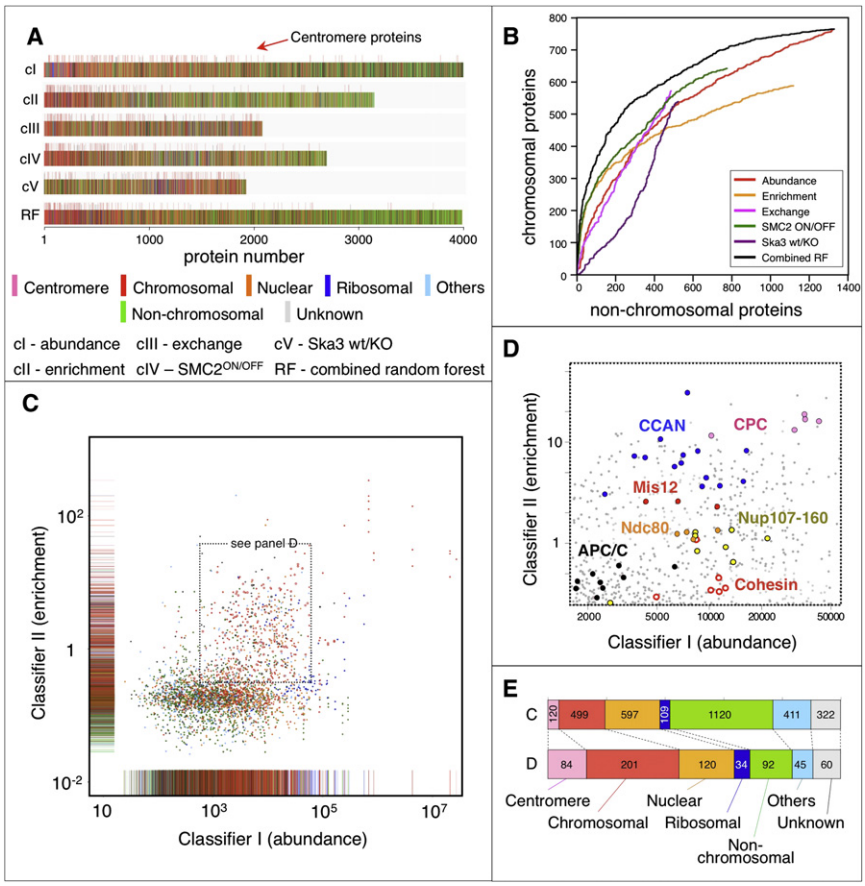

Figure 2. Combining Classifiers Increases Specificity

(A) The rank of all proteins observed for proteomic classifiers I (abundance), II (enrichment), III (retention), IV (SMC2 dependency), V (Ska3/Rama1 dependency) and RF (combined random forest ranking) is plotted as vertical color coded lines (rug plots). Proteins are ranked from the highest (left) to lowest values for each classifier. Centromere proteins are indicated by longer bars (indicated).

(B) Cumulative curves show that combining classifiers by RF significantly increases the specificity of identifying chromosomal proteins without compromising the completeness of the analysis.

(C) 2D scatter graph plotting classifiers I versus II flanked by the relevant rug plots. Proteins most enriched in chromosomes relative to cytoplasm and proteins most abundant in chromosomes are above and to the right, respectively. Each spot is color-coded by category (Figure 1D).

(D) Zoom of the region indicated in (C) showing members of the chromosomal passenger (CPC), Mis12, Ndc80, Nup107-160 and Cohesin complexes plus the constitutive centromere-associated network (CCAN) and anaphase-promoting complex/cyclosome (APC/C).

(E) Enrichment for chromosomal proteins in the region indicated in (C & D).

See also Figure S2.

isolated (Figure 1E). Classifier IV is the heavy/light ratio ($SMC2^{ON}/SMC2^{OFF}$) for each of the proteins identified in this experiment.

SMC2-depleted chromosomes contained 5.8% of the wild-type level of SMC2. It is not possible to isolate chromosomes from cultures completely lacking SMC2 as *SMC2* is an essential gene and dead cells do not accumulate in mitosis. These chromosomes were similarly depleted of all condensin I and II subunits.

Classifier V: Ska3/Rama1 Dependency

To demonstrate the targeted analysis possible with our approach, we compared the association of kinetochore proteins with chromosomes in cells with or without Ska3/Rama1/C13orf3. Ska3/Rama1, which was identified in this analysis as a chromosomal protein, was described in several recent publications (Daum et al., 2009; Gaitanos et al., 2009; Raaijmakers et al., 2009; Theis et al., 2009; Welburn et al., 2009).

To obtain chromosomes depleted of Ska complex, we isolated a genetic knockout of the *Ska3/Rama1* gene (Figures S5A and S5B). *Ska3/Rama1*$^{-/-}$ cells (homozygous knockouts are viable) were grown in $SILAC^{light}$ medium (Figure 1E). Equal numbers of *Ska3/Rama1*$^{-/-}$ and wild-type DT40 (cultured in $SILAC^{heavy}$ medium) mitotic cells from the two different populations were mixed and mitotic chromosomes isolated. Classifier V is the heavy/light ratio (wild-type/*Ska3/Rama1*$^{-/-}$) for each protein identified in this experiment.

Classifier VI: Domain Analysis

We added an additional nonproteomic classifier to our analysis using the protein domains found in chromosomal and nonchromosomal proteins (red/pink and green wedges in Figure 1D). This made use of bioinformatic analysis in order to segregate chromosomal from nonchromosomal proteins, but importantly did not consider a protein's relevance to mitosis. We counted how often each domain was observed in chromosomal and nonchromosomal proteins and assigned it this frequency as a score (Table S2). Classifier VI was then determined for each protein based on the sum of its domain scores.

Multiclassifier Combinatorial Proteomics

Traditional one-dimensional analysis (e.g., sorting the various proteins according to their value for each classifier) was of limited utility, as the data lacked a clear boundary between chromosomal (red/pink in Figure 2A) and nonchromosomal proteins (green in Figure 2A) for each classifier (Figure 2A and Figures S2A–S2E).

By contrast, when classifiers were combined, our ability to identify chromosomal proteins was vastly improved. For example, an enrichment of centromeric or chromosomal proteins relative to nonchromosomal proteins was obtained when classifiers I (abundance) and II (enrichment) were plotted (Figures 2C–2E). The clustering of protein complex subunits in this plot (Figure 2D) reflects both their relative stoichiometry

(*x* axis), and the similar degree to which subunits in a complex are all present either on or off chromosomes (*y* axis). Members of the APC/C, Ndc80 and Mis12 complexes form closely knit clusters. It is important to note that this was achieved in the context of entire chromosomes and without requiring solubilization of the complexes.

We used random forest (RF) analysis, a machine learning approach, to progress beyond two-dimensional analyses and integrate the information present in all proteomics classifiers. This analysis offered two powerful benefits. First, it enabled us to work with data sets that contain missing values. This is a significant advantage in proteomics studies where not every protein is observed in every experiment, as seen in Figure 2A and Figure S2F. Second, RF analysis allowed us to use any descriptor of our proteins as a classifier and integrate it into our overall analysis. Here, we also included a bioinformatic analysis of the distribution of protein domains in our analysis distinguishing chromosomal from nonchromosomal proteins (classifier VI).

In brief, RF is a decision tree analysis that separates data sets into ''true'' and ''false'' groups. The decision trees are trained on defined data sets and randomly built to optimize the separation between them. Analysis of the experimental data set then occurs by running each protein through all trees and adding up its overall RF score (i.e., the fraction of trees that scored it as ''true''). RFs perform much better on training data than application data, so their performance is evaluated by ten-fold cross-validation. The training data are split into random sections of 90% for training and 10% for evaluation, so that successively the entire set is used for evaluation. Here, the two training data sets chosen were ''nonchromosomal'' (green wedges in Figure 1D) and ''chromosomal'' (red + pink wedges in Figure 1D), and the RF score for a given protein is the fraction of trees that scored it as ''chromosomal.''

RF analysis readily discriminated chromosomal from nonchromosomal proteins. In the RF rug plot of Figure 2A, which represents the ranked list of proteins generated by RF analysis, the left side is predominantly red, while the right side is predominantly green. To reach the 500th chromosomal protein on the RF-ranked list only 229 nonchromosomal proteins are included (Figure 2B). In contrast, 410-671 nonchromosomal proteins would be included when considering ranked lists from individual classifiers. Note that the RF-based sorting was done on the complete data set, including proteins that failed to be observed with some classifiers. Therefore, adding information from additional experiments did not decrease the number of proteins covered.

The advantage of combining classifiers can be statistically expressed by ROC curves (Figure S3A), with increased area under the curve (AUC) for our combined analysis when compared to each of the individual classifiers ($AUC^{RF(cI-V)}$ = 0.81, $AUCs^{cI-V}$ = 0.41-0.76). The combined classifiers assigned 88.8% of our gold standard, the 125 centromere proteins, correctly as chromosomal, at the cut-off that minimizes misassignment of chromosomal versus nonchromosomal proteins. This specificity was further improved when bioinformatic domain analysis (cVI) was integrated with our proteomic classifiers ($AUC^{RF(cI-VI)}$ = 0.97; identification of the first 500 chromosomal proteins yields 17 nonchromosomal proteins, Suppl. Figures S3B and S3C, proteins lacking known domains are excluded from this boost, Figure S3D). Now, 92.4% of the centromere proteins were assigned as chromosomal. In summary, RF analysis provides us with a tool for productively combining the outcomes of our individual proteomics classifier experiments and further empowering our analysis by including data from other sources.

If results of a random forest based on the five proteomic classifiers plus the bioinformatics-based classifier VI were plotted against those from the initial random forest analysis (Figure 3A), a near-perfect separation of the training data was achieved. Only a single chromosomal protein of the training set and two nonchromosomal proteins were misassigned when placing manually a separation line.

Using ten-fold cross-validation, we found that 118 centromere proteins positioned right and only 7 left of the separation line (Figure 3B). This compares to 14 and 9 centromere proteins being missed when using the one-dimensional ranked lists by classifiers I-V and I-VI, respectively. Accepting the line as a threshold returns known centromere proteins with a yield of 94.4% and all other chromosomal proteins with 93.1% success. In contrast, 83.1% of nonchromosomal proteins are rejected. Thus, the classifier approach is sufficiently powerful to suggest chromosomal proteins from among hitherto uncharacterized proteins.

Identification of New Chromosomal Proteins

To test the predictive power of our RF analysis, we cloned and tested the location in mitosis of 50 previously uncharacterized proteins including 15 without known domains: 34 predicted to be and 16 predicted not to be on chromosomes in mitosis.

Reasoning that important proteins would be conserved, we expressed GFP-tagged human homologs of these chicken proteins in U2OS cells. Remarkably, 30 of 34 cloned proteins from the chromosomal region were confirmed as chromosomal, contrasting with only 2 of the 16 predicted *ab initio* to be nonchromosomal. This confirms the power of our analysis and indicates a success rate of 88%, with 44 of 50 tagged proteins localizing as predicted. Of 50 newly cloned proteins, 13 were associated with kinetochores in mitosis, 12 had a more general distribution on mitotic chromosomes and 7 others were perichromosomal, a class whose new members we propose to term *c*hromosome *peri*phery proteins (cPERPs A-G) (Figures S4B–S4G and Table S3). The chromosome periphery (perichromosomal layer) is enriched in ribosomal and nucleolar hitchhiker proteins, and is of unknown function (Van Hooser et al., 2005).

The new centromere proteins all appeared to localize to the outer kinetochore, relative to CENP-C and HEC1 as standards (Figures 4B–4J, Figure S4A). In keeping with established nomenclature, we propose to name these proteins CENP-Y, CENP-Z and CENP-27 through CENP-33. Beyond 'Z', the 26th letter of the basic modern Latin alphabet, we propose to designate the new proteins with numbers starting with CENP-27.

Functional Analysis of New Kinetochore-Associated Proteins

We focused our initial functional analysis on kinetochore proteins. Clustering analysis (Gentleman et al., 2004) allowed us to combine data for proteins identified by all classifiers, and

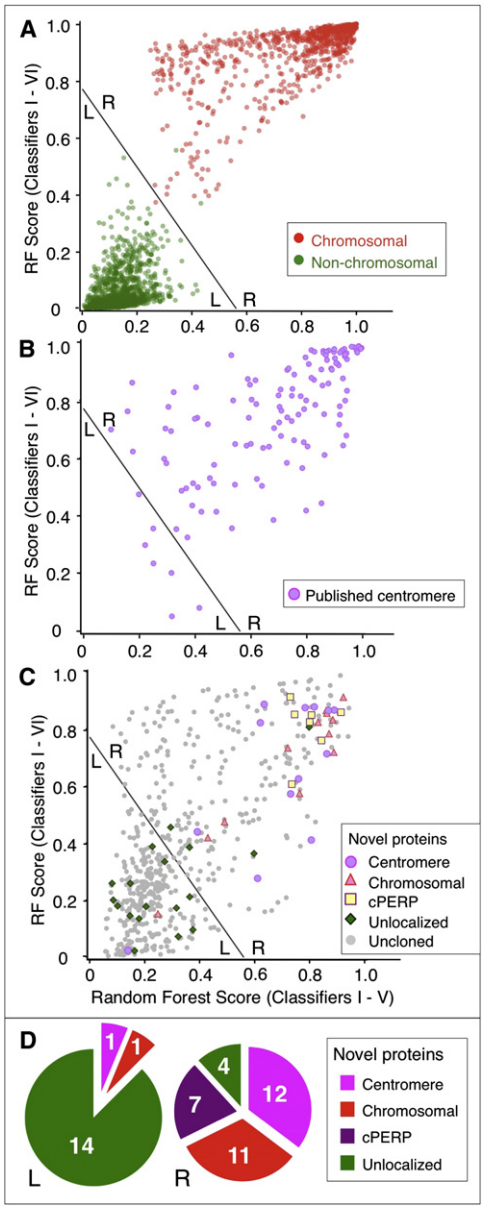

Figure 3. Random Forest Analysis Predicts New Proteins of Interest

(A) Separation of the two training sets (color-coded groups from Figure 1D) by RF analysis. The line provides optimal separation of the two training sets. x axis: RF analysis of classifiers I–V; y axis: RF analysis of classifiers I–VI, including the bioinformatic domain analysis.

(B) Positions of previously known centromere proteins from ten-fold cross-validation.

(C) Position of cloned proteins and remaining uncloned proteins in the same 2d analysis.

(D) Classification of newly cloned proteins from regions to the left and right of the dividing line, respectively.

See also Figure S3.

look for informative groupings. This revealed a striking tendency for functionally related proteins to form clusters, as exemplified by members of the NDC80, CPC, Nup107-160 and APC/C complexes (Figure 4). Interestingly, our clustering sorted CENP-27 as a component of the APC/C. This was confirmed and the protein named APC16 in three recent reports (Hutchins et al., 2010; Kops et al., 2010; Hubner et al., 2010). To further test the predictive value of cluster analysis for proteomic data sets, we examined two kinetochore proteins in greater detail.

Ska3/Rama1 and Functional Analysis of Kinetochore Subcomplexes

C13orf3 was located adjacent to Ska2 in the cluster analysis. This protein now known as Ska3/Rama1 has been suggested to be involved in microtubule attachment to kinetochores (Gaitanos et al., 2009; Raaijmakers et al., 2009; Welburn et al., 2009) or coordination of the spindle checkpoint response (Daum et al., 2009; Theis et al., 2009). We analyzed the kinetochore proteome in the presence or absence of Ska3/Rama1 (defined as classifier V) in order to determine the role of this protein in kinetochore structure (Figure 5).

A map of the *Ska3/Rama1* locus in DT40 is shown in Figures S5A and S5B, together with a targeting strategy for inactivating the gene. The *Ska3/Rama1* gene is not essential for life in DT40 cells (Figure S5C). However, these cells struggle to achieve a normal chromosome alignment, and show a ~3× increase in mitotic index (Figure S5D and S5E), a ~3× increase in the percentage of apoptotic cells and a ~6x increase in the number of bi-nucleated cells.

Proteomic analysis of isolated chromosomes revealed that loss of Ska3/Rama1 was accompanied by the loss of Ska1 and Ska2. Loss of the Ska complex caused no systematic changes in the chromosomal association of proteins of the constitutive centromere-associated network (CCAN), Knl-1/Mis12/Ndc80 (KMN), Mis18, Ndc80, CPC, and Nup107-160 kinetochore subcomplexes. However, striking changes were seen in the levels of the APC/C, RanBP2/RanGAP1, spindle checkpoint, Rod/Zw10/Zwilch (RZZ), and dynein/dynactin complexes. We confirmed that the RanBP2/RanGAP1 complex is indeed depleted from kinetochores when *Ska3/Rama1* is deleted in HeLa cells (Figure S5F and S5G). Attempts to confirm the specific kinetochore depletion of the APC/C were uninformative, as we were unable to reproducibly obtain kinetochore staining for the APC/C in HeLa cells using four independent antibodies.

We conclude that combining genetic and SILAC analysis provides a powerful new method for analysis of multicomplex protein superstructures.

A Protein Involved in Chromosome Alignment and Spindle Organization

A second new kinetochore-associated protein, CENP-32/C9orf114, was sorted on our kinetochore cluster diagram next to CLASP1 and CLASP2, two paralogues known to be involved in the regulation of microtubule dynamics. Like CLASPs, CENP-32/C9orf114 mapped to the outer kinetochore (Figure 6A), and its depletion caused a significant accumulation of cells in later prometaphase (Figure S6A) with misaligned chromosomes (Figure 6B). These cells frequently had bipolar spindles, however 60% of those spindles exhibited remarkable abnormalities where centrosomes appeared to have detached from the poles (Figures 6C and 6D and Figure S6B). In one remarkable case, the centrosomes appeared at the midzone of a bipolar spindle (Figure 6C[9-12]).

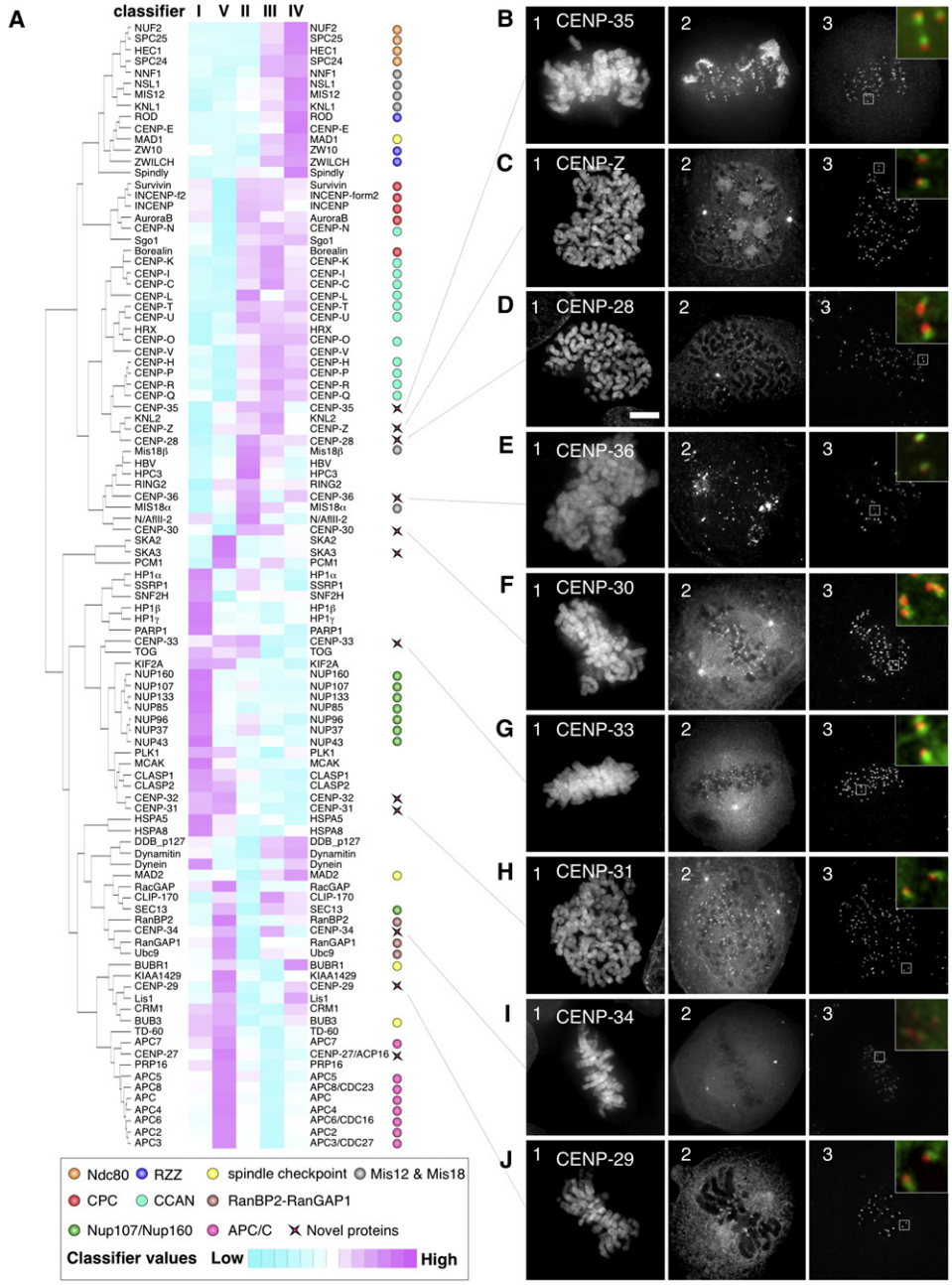

Figure 4. Cluster Analysis and Imaging of New Kinetochore Proteins

(A) Heat map and cluster dendrogram for 101 centromere-associated proteins identified by all 5 proteomic classifiers. Known complexes are color-marked (see bottom) and show a tendency to cluster in this analysis. Kinetochore proteins identified in this study are also marked (stars).

(B–J) Localization of GFP-tagged kinetochore-associated proteins (panels 2) relative to DNA detected with DAPI (panels 1) and CENP-C (panels 3 in [B]–[D], [F]–[H], and [J] or ACA (panels 3 in [E] and [I]). Insets show merged images with blow-ups of representative kinetochores (GFP-novelCENP, green and CENP-C or ACA, red).

See also Figure S4.

DISCUSSION

Multiclassifier Combinatorial Proteomics

The approach described here for analysis of the proteome of vertebrate mitotic chromosomes can be used to study any complex proteome. The key approach of combining classifier data can in principle be expanded indefinitely and can include nonproteomics data sets such as the bioinformatic protein domain analysis used here. Other classifiers that could be used in the future include microarray, protein interaction

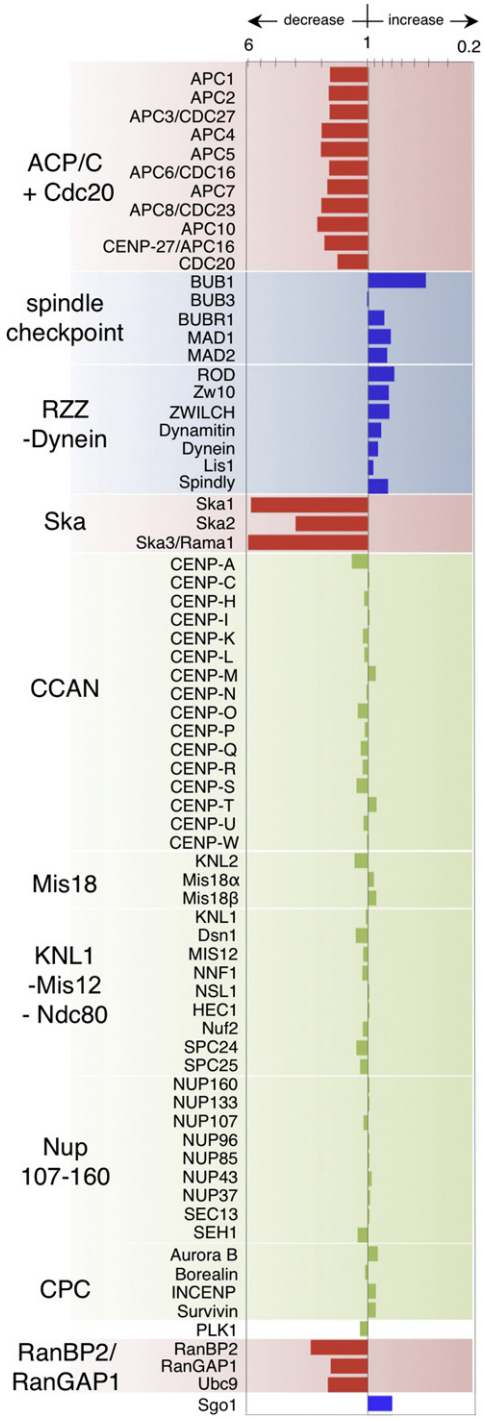

Figure 5. Ska3/Rama1 Dependency for Chromosomal Association and Analysis of CENP-27/APC16

Kinetochore proteins with increased abundance on chromosomes in the absence of Ska3/Rama1 are shown with blue bars and proteins with decreased abundance are shown with red bars. Note covariance of protein complexes. See also Figure S5.

(e.g., two hybrid screens or pull-down), protein phosphorylation, and localization data and, indeed, data from any experimental approach in which the proteins of interest are sorted systematically.

We first showed that plotting pairs of classifiers against one another improved our ability to delineate potential chromosomal proteins. As that approach could not be generalized when the number of classifiers exceeded three, we adopted a random forest (RF) analysis approach. This allowed us to integrate information from all classifiers into decision trees on which known and unknown proteins could be classified. Importantly, RF analysis handles missing values systematically. This is crucial when not every protein is observed in every experiment. In contrast, cluster analysis, which has been used both in this study and in other recent work (Theis et al., 2009; Neumann et al., 2010), can only integrate data for proteins that have a value for every classifier.

Integrity of the Isolated Chromosomes

Our methods focused on optimizing the purity of the chromosomes. Thus, our list of proteins is likely to represent the minimal, stably associated components of mitotic chromosomes. Nonetheless kinetochores of isolated chromosomes retain some function, as judged by their ability to recruit components of the mitotic checkpoint complex from cytoplasm. This may be because chromosomes were isolated from nocodazole-treated cells, with kinetochores actively engaged in spindle checkpoint signaling.

New Insights into Kinetochore Functional Organization

Remarkably, although no biochemical enrichment for centromeres was performed, our data set contained all known centromeric subcomplexes, with peptides from 125 reported centromere proteins (eight present as multiple isoforms) (Table S1). We identified all members of the CCAN, KMN, Mis12 and Mis18 complexes and all members of the RZZ complex except Zwint (which is not yet annotated in the chicken genome). Our success in identifying centromere and telomere proteins may be explained because 66 of the 78 chicken DT40 chromosomes are microchromosomes whose purification provides a natural enrichment for centromeres and telomeres since the chromosome arms are so short.

We combined genetics with whole proteome analysis in order to identify complexes and structural dependencies in their "native environment" (e.g., kinetochore proteins in actual kinetochores). Chromosomes lacking Ska3/Rama1 were depleted for the entire Ska complex, confirming that these three proteins are interdependent for chromosome binding. Similarly, depletion of key condensin subunit SMC2 caused a loss of all seven subunits of the condensin I and II complexes from chromosomes. Importantly, this analysis did not require tagging of any proteins or attempts to solubilize functional complexes from large subcellular structures.

In addition to these primary effects of depletion, loss of Ska3/Rama1 also caused a significant secondary depletion of the APC/C and RanBP2/RanGAP1 complexes from chromosomes but had no consistent effect on most other kinetochore proteins. Importantly, all members of the secondary-depleted complexes

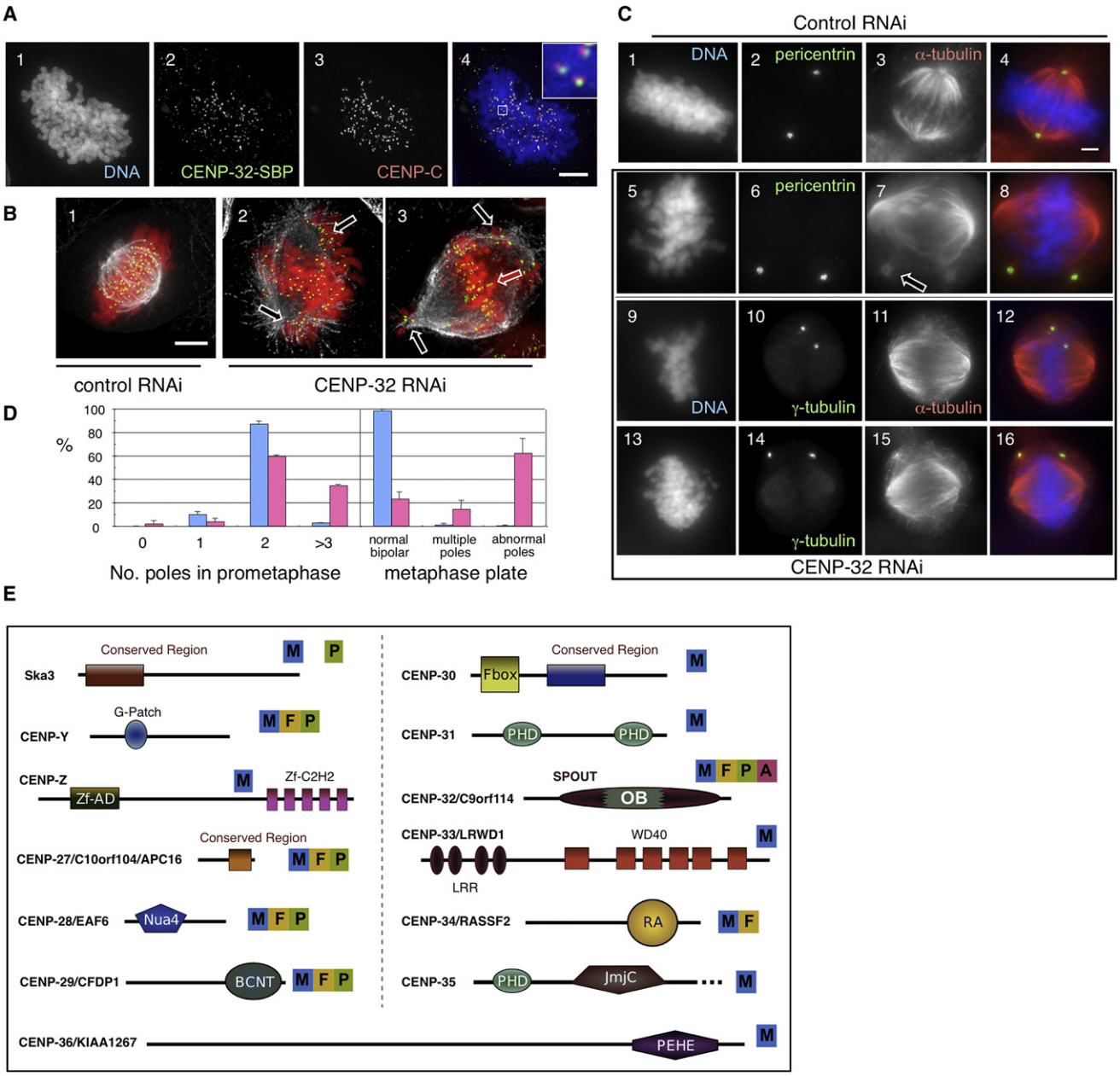

Figure 6. Initial Characterization of CENP-32

(A) Localization of GFP-CENP-32 (panel 2, green) in the kinetochore relative to DNA (panel 1, blue) and CENP-C (panel 3, red).

(B) CENP-32 RNAi causes problems with chromosome alignment. DNA, red; CENP-C, green; microtubules, white.

(C) CENP-32 RNAi causes detachment of centrosomes from bipolar spindles. DNA (panels 1,5,9,13), blue; pericentrin (panels 2,6) or γ-tubulin (panels 10,14), green; α-tubulin (panels 3,7,11,15), red.

(D) Quantitation of spindle phenotypes following CENP-32 RNAi.

(E) Schematic representation of domain architectures for new kinetochore proteins tagged in this study (drawn to approx. scale). The locations of domains are according to Pfam and SMART family databases (Letunic et al., 2004; Finn et al., 2010), complemented by REP web server analysis (Andrade et al., 2000). The localization of the PEHE domain has been assigned from (Marín, 2003). Phyletic distributions of proteins are indicated in blue, yellow, green and violet for Metazoa, Fungi, Plantae and Archaea, respectively. CENP-35 has been truncated. Abbreviations: BCNT, Bucentaur or craniofacial development protein; Fbox, cyclin-F motif; G-Patch, Glycine-rich nucleic binding domain; JmjC, jumonji C domain; LRR, Leucine-rich repeats; Nua4, Nucleosomal acetyltransferase of H4; OB, Oligonucleotide/oligosaccharide Binding; PEHE, Pro-Glu-His-Glu conserved region; PHD, Plant HomeoDomain; RA, Ras associated (RalGDS/AF-6) domain; SPOUT, spoU and trmD RNA methyltransferase; WD40, WD/beta-transducin repeats; Zf-AD, Zinc finger-associated domain; and Zf-C2H2, Classical zinc finger Cys(2)His(2).

See also Figure S6.

also behaved coordinately. Our results (e.g., the behavior of CENP-27/APC16 as a component of the APC/C) confirm the utility of single protein depletion analysis for the identification of protein complexes and determination of their mutual interdependencies for association with chromosomes.

Our data suggest that the Ska complex may provide a docking site for the APC/C in the outer kinetochore. Alternatively, sumoylation by RanBP2 may have a role in APC/C binding to chromosomes. The RanBP2-RanGAP1 complex is known to be involved in kinetochore-microtubule interactions and localization of several spindle checkpoint proteins (Joseph et al., 2004). We note that among the recent spate of publications on Ska3/Rama1, our observations appear to support a role in integration and regulation of the spindle checkpoint response (Daum et al., 2009; Theis et al., 2009).

Our whole-proteome analysis revealed that Cdc20 behaved like a member of the APC/C and was distinct from other components of the spindle checkpoint pathway with respect to its Ska complex dependency. Spindle checkpoint components associate with one another in cytoplasm as a mitotic checkpoint complex (MCC), containing BubR1, Bub3, Cdc20 and Mad2. Our data suggest that once the MCC associates with chromosomes, Cdc20 stably associates with the APC/C.

What Classes of Kinetochore Proteins Remain to Be Discovered?

We identified 13 kinetochore-associated proteins among previously uncharacterized proteins and, as discussed below, we predict that many more remain to be described. We therefore asked whether there is any functional relationship between these new proteins. That is, what sorts of kinetochore proteins had been missed in the many previous genetic and biochemical screens? An interesting answer has emerged.

Since the new kinetochore proteins were identified solely based on their occurrence in chromosomes, they could potentially represent a wide range of functions. Nevertheless, it is striking that five of the new centromere proteins (namely, CENP-28, −29, −31, −35, and −36) are subunits of complexes that modify and/or bind histones (Figure 6E). Yeast orthologs of two of these proteins (namely, CENP-28/C1orf149 and CENP-29/CFDP1) contribute to NuA4 histone acetyltransferase (HAT) and SWR1 ATP-dependent chromatin remodelling complexes, respectively. These complexes are known to share components (Wu et al., 2005) and together stimulate the exchange of histone H2A for H2A.Z, following acetylation of H2A or H4 (Altaf et al., 2010). A third centromere-associated protein, CENP-36/MSL1v1, is necessary for the activity of MOF, another HAT, on nucleosomal H4 (Li et al., 2009). Finally, CENP-31/PHD6 and CENP-35/PHF2 each contain PHD (plant homeodomain) zinc fingers, which are usually associated with chromatin-mediated transcriptional regulation. The PHD of CENP-35, which also contains a JmjC (likely histone demethylase) domain, appears to be required for demethylation of H3 at the promoters of ribosomal RNA genes (Wen et al., 2010).

Why were these proteins not discovered earlier as kinetochore-associated? One likely explanation is that they may have essential functions in other chromatin regions as well. Thus, mutations might have pleiotropic phenotypes not recognized as specific for mitosis. Furthermore, their association might depend on a fully assembled kinetochore and thus be lost when attempting other than whole chromosome analysis.

Characterization of a Kinetochore Protein

CENP-32 is required both for chromosome alignment and for association of the centrosomes with the poles of the bipolar spindle during metaphase. This latter phenotype is very similar to an unusual spindle morphology phenotype seen in *Drosophila* cells following depletion of the CLASP homolog Mast/Orbit (Maiato et al., 2002). Indeed, in our analysis, CENP-32 clusters with CLASP1 and CLASP2. A yeast homolog of CENP-32 interacts with CBF5, an enzyme involved in the posttranscriptional modification of rRNA, that was shown to bind to budding yeast centromeres and microtubules (Jiang et al., 1993). Bioinformatics analysis suggests that CENP-32 is a member of the SPOUT family of methyltransferases but is atypical in possessing a possible RNA-binding OB fold inserted into its catalytic domain (Tkaczuk et al., 2007). It is tempting to speculate that CENP-32 may function at kinetochores by interacting with an as-yet unknown RNA.

How Complex Is the Kinetochore?

MCCP analysis allows us to predict how many more kinetochore proteins remain to be identified in our data set. In the plot of Figure 3, where the chromosomal proteome is displayed in two dimensions, we found 35% of novel tagged proteins from region R and 6% from region L to associate with the kinetochore during mitosis. These regions have 224 and 287 as-yet uncharacterized novel proteins, respectively. Assuming no bias in the proteins we cloned, this suggests that approximately 97 more kinetochore proteins remain to be discovered. Taking into account the 13 kinetochore-associated proteins confirmed in our work, this roughly doubles the currently known protein complexity of the kinetochore during mitosis, confirming it as one of the most complex cellular substructures.

Conclusions

Multiclassifier combinatorial proteomics and the data sets described here open the door to the identification of all functional components of mitotic chromosomes despite the adventitious binding of cellular background proteins during mitosis. Furthermore, MCCP can be extended by adding additional classifiers to delineate protein complexes and define functional dependencies between them in the context of intact mitotic chromosomes. This will serve both as a starting point for systematic determination of the full range of functions involved in mitotic chromosome segregation, and as a basis for the development of detailed structural and functional interaction maps of key chromosomal subdomains. MCCP should also prove useful for the analysis of other cellular structures that lack defined boundaries, e.g., membrane associated complexes like the post-synaptic density.

EXPERIMENTAL PROCEDURES

Preparation of Mitotic Chromosomes

DT40 cells were incubated with Nocodazole for 13 hr, resulting in a mitotic index of 70%–90%. Mitotic chromosomes were isolated in the polyamine-EDTA buffer system optimized for chicken DT40 cells (Lewis and Laemmli,

1982). 19.3 OD_{260} units were obtained from pooling the material of four independent preparations totaling 7.5 × 10^9 DT40 cells and solubilized in SDS-polyacrylamide gel electrophoresis (SDS-PAGE) sample buffer.

Preparation of Chromosome-Free Mitotic Cell Extracts

Nocodazole blocked DT40 cells were dounce-homogenized under hypotonic conditions. Mitotic chromosomes were removed by centrifuging the supernatant twice at 10,000 x g and discarding the pellets to prepare a cell extract free of chromosomes.

To measure the ratios between chromosomal and nonchromosomal proteins, SILAC based mass spectrometry was performed with 150 μg of labeled cell extract from 7.0 × 10^6 cells and 150 μg of nonlabeled proteins contained in isolated chromosomes from 2.0 × 10^9 cells.

To measure the exchange ratio, we isolated mitotic chromosomes from roughly 1.0 × 10^9 cells. Mitotic chromosomes were pelleted after centrifuging at 3000 × g and mixed into 10 ml cell extract that were made from 3.0 × 10^8 cells. This mixture was incubated at 14°C for 30 min. Finally, we re-isolated the chromosomes as described above.

Mass Spectrometric Analysis

Proteins were separated into a high and a low molecular weight fraction by SDS-PAGE, in-gel digested using trypsin (Shevchenko et al., 2006), and fractionated into 30 fractions each using SCX. The individual SCX fractions were desalted using StageTips (Rappsilber et al., 2003) and analyzed using LC-MS on a LTQ-Orbitrap (Thermo Fisher Scientific) coupled to HPLC via a nanoelectrospray ion source. The six most intense ions of a full MS acquired in the orbitrap analyzer were fragmented and analyzed in the linear ion trap. The MS data were analyzed using MaxQuant (Cox and Mann, 2008) and proteins identified by searching MS and MS/MS data using the MASCOT search engine (Matrix Science, UK). For more details, see the Extended Experimental Procedures.

SUPPLEMENTAL INFORMATION

Supplemental Information includes Extended Experimental Procedures, six figures, and five tables and can be found with this article online at doi:10.1016/j.cell.2010.07.047.

ACKNOWLEDGMENTS

We dedicate this paper to Uli Laemmli on the occasion of his 70th birthday. We thank Mayumi Takahashi for assistance with preparation of the *Ska3/Rama1* knockout, Frauke Melchior for anti-RanBP2 and David Tollervey, Margarete Heck, Robin Allshire, Iain Cheeseman, Kumiko Samejima, Susana Ribeiro and Jan Bergmann for critical reading of the manuscript. This work was supported by a European Community Marie Curie Excellence Grant (JR), the MRC (CPP), EMBO (LSP) and the Wellcome Trust (WCE, JR). WCE and JR are Principal and Senior Research Fellows of The Wellcome Trust, respectively.

Received: December 7, 2009
Revised: May 20, 2010
Accepted: July 14, 2010
Published: September 2, 2010

REFERENCES

Altaf, M., Auger, A., Monnet-Saksouk, J., Brodeur, J., Piquet, S., Cramet, M., Bouchard, N., Lacoste, N., Utley, R.T., Gaudreau, L., et al. (2010). NuA4-dependent acetylation of nucleosomal histone H4 and H2A directly stimulates incorporation of H2A.Z by the SWR1 complex. J. Biol. Chem., in press.

Amano, M., Suzuki, A., Hori, T., Backer, C., Okawa, K., Cheeseman, I.M., and Fukagawa, T. (2009). The CENP-S complex is essential for the stable assembly of outer kinetochore structure. J. Cell Biol. *186*, 173–182.

Andersen, J.S., Wilkinson, C.J., Mayor, T., Mortensen, P., Nigg, E.A., and Mann, M. (2003). Proteomic characterization of the human centrosome by protein correlation profiling. Nature *426*, 570–574.

Andrade, M.A., Ponting, C.P., Gibson, T.J., and Bork, P. (2000). Homology-based method for identification of protein repeats using statistical significance estimates. J. Mol. Biol. *298*, 521–537.

Cheeseman, I.M., and Desai, A. (2008). Molecular architecture of the kinetochore-microtubule interface. Nat. Rev. Mol. Cell Biol. *9*, 33–46.

Cox, J., and Mann, M. (2008). MaxQuant enables high peptide identification rates, individualized p.p.b.-range mass accuracies and proteome-wide protein quantification. Nat. Biotechnol. *26*, 1367–1372.

Daum, J.R., Wren, J.D., Daniel, J.J., Sivakumar, S., McAvoy, J.N., Potapova, T.A., and Gorbsky, G.J. (2009). Ska3 is required for spindle checkpoint silencing and the maintenance of chromosome cohesion in mitosis. Curr. Biol. *19*, 1467–1472.

de Godoy, L.M., Olsen, J.V., Cox, J., Nielsen, M.L., Hubner, N.C., Frohlich, F., Walther, T.C., and Mann, M. (2008). Comprehensive mass-spectrometry-based proteome quantification of haploid versus diploid yeast. Nature *455*, 1251–1254.

Dejardin, J., and Kingston, R.E. (2009). Purification of proteins associated with specific genomic Loci. Cell *136*, 175–186.

Earnshaw, W.C., and Rothfield, N. (1985). Identification of a family of human centromere proteins using autoimmune sera from patients with scleroderma. Chromosoma (Berl) *91*, 313–321.

Finn, R.D., Mistry, J., Tate, J., Coggill, P., Heger, A., Pollington, J.E., Gavin, O.L., Gunasekaran, P., Ceric, G., Forslund, K., et al. (2010). The Pfam protein families database. Nucleic Acids Res. *38*, D211–D222.

Foltz, D.R., Jansen, L.E., Black, B.E., Bailey, A.O., Yates, J.R., and Cleveland, D.W. (2006). The human CENP-A centromeric nucleosome-associated complex. Nat. Cell Biol. *8*, 458–469.

Foster, L.J., De Hoog, C.L., and Mann, M. (2003). Unbiased quantitative proteomics of lipid rafts reveals high specificity for signaling factors. Proc. Natl. Acad. Sci. USA *100*, 5813–5818.

Gaitanos, T.N., Santamaria, A., Jeyaprakash, A.A., Wang, B., Conti, E., and Nigg, E.A. (2009). Stable kinetochore-microtubule interactions depend on the Ska complex and its new component Ska3/C13Orf3. EMBO J. *28*, 1442–1452.

Gassmann, R., Henzing, A.J., and Earnshaw, W.C. (2005). Novel components of human mitotic chromosomes identified by proteomic analysis of the chromosome scaffold fraction. Chromosoma *113*, 385–397.

Gentleman, R.C., Carey, V.J., Bates, D.M., Bolstad, B., Dettling, M., Dudoit, S., Ellis, B., Gautier, L., Ge, Y., Gentry, J., et al. (2004). Bioconductor: open software development for computational biology and bioinformatics. Genome Biol. *5*, R80.

Hori, T., Amano, M., Suzuki, A., Backer, C.B., Welburn, J.P., Dong, Y., McEwen, B.F., Shang, W.H., Suzuki, E., Okawa, K., et al. (2008). CCAN makes multiple contacts with centromeric DNA to provide distinct pathways to the outer kinetochore. Cell *135*, 1039–1052.

Hubner, N.C., Bird, A.W., Cox, J., Splettstoesser, B., Bandilla, P., Poser, I., Hyman, A., and Mann, M. (2010). Quantitative proteomics combined with BAC TransgeneOmics reveals in vivo protein interactions. J. Cell Biol. *189*, 739–754.

Hudson, D.F., Vagnarelli, P., Gassmann, R., and Earnshaw, W.C. (2003). Condensin is required for nonhistone protein assembly and structural integrity of vertebrate mitotic chromosomes. Dev. Cell *5*, 323–336.

Hutchins, J.R., Toyoda, Y., Hegemann, B., Poser, I., Heriche, J.K., Sykora, M.M., Augsburg, M., Hudecz, O., Buschhorn, B.A., Bulkescher, J., et al. (2010). Systematic analysis of human protein complexes identifies chromosome segregation proteins. Science *328*, 593–599.

Ishihama, Y., Oda, Y., Tabata, T., Sato, T., Nagasu, T., Rappsilber, J., and Mann, M. (2005). Exponentially modified protein abundance index (emPAI) for estimation of absolute protein amount in proteomics by the number of sequenced peptides per protein. Mol. Cell. Proteomics *4*, 1265–1272.

Ishihama, Y., Schmidt, T., Rappsilber, J., Mann, M., Hartl, F.U., Kerner, M.J., and Frishman, D. (2008). Protein abundance profiling of the Escherichia coli cytosol. BMC Genomics *9*, 102.

Jiang, W., Middleton, K., Yoon, H.J., Fouquet, C., and Carbon, J. (1993). An essential yeast protein, CBF5p, binds in vitro to centromeres and microtubules. Mol. Cell. Biol. *13*, 4884–4893.

Joseph, J., Liu, S.T., Jablonski, S.A., Yen, T.J., and Dasso, M. (2004). The RanGAP1-RanBP2 complex is essential for microtubule-kinetochore interactions in vivo. Curr. Biol. *14*, 611–617.

Kops, G.J., van der Voet, M., Manak, M.S., van Osch, M.H., Naini, S.M., Brear, A., McLeod, I.X., Hentschel, D.M., Yates, J.R., 3rd, van den Heuvel, S., and Shah, J.V. (2010). APC16 is a conserved subunit of the anaphase-promoting complex/cyclosome. J. Cell Sci. *123*, 1623–1633.

Kulukian, A., Han, J.S., and Cleveland, D.W. (2009). Unattached kinetochores catalyze production of an anaphase inhibitor that requires a Mad2 template to prime Cdc20 for BubR1 binding. Dev. Cell *16*, 105–117.

Letunic, I., Copley, R.R., Schmidt, S., Ciccarelli, F.D., Doerks, T., Schultz, J., Ponting, C.P., and Bork, P. (2004). SMART 4.0: towards genomic data integration. Nucleic Acids Res. *32*, D142–D144.

Lewis, C.D., and Laemmli, U.K. (1982). Higher order metaphase chromosome structure: evidence for metalloprotein interactions. Cell *29*, 171–181.

Li, X., Wu, L., Corsa, C.A., Kunkel, S., and Dou, Y. (2009). Two mammalian MOF complexes regulate transcription activation by distinct mechanisms. Mol. Cell *36*, 290–301.

Maiato, H., Sampaio, P., Lemos, C.L., Findlay, J., Carmena, M., Earnshaw, W.C., and Sunkel, C.E. (2002). MAST/Orbit has a role in microtubule-kinetochore attachment and is essential for chromosome alignment and maintenance of spindle bipolarity. J. Cell Biol. *157*, 749–760.

Marín, I. (2003). Evolution of chromatin-remodeling complexes: comparative genomics reveals the ancient origin of "novel" compensasome genes. J. Mol. Evol. *56*, 527–539.

Morrison, C., Henzing, A.J., Jensen, O.N., Osheroff, N., Dodson, H., Kandels-Lewis, S.E., Adams, R.R., and Earnshaw, W.C. (2002). Proteomic analysis of human metaphase chromosomes reveals topoisomerase II alpha as an Aurora B substrate. Nucleic Acids Res. *30*, 5318–5327.

Neumann, B., Walter, T., Heriche, J.K., Bulkescher, J., Erfle, H., Conrad, C., Rogers, P., Poser, I., Held, M., Liebel, U., et al. (2010). Phenotypic profiling of the human genome by time-lapse microscopy reveals cell division genes. Nature *464*, 721–727.

Obuse, C., Iwasaki, O., Kiyomitsu, T., Goshima, G., Toyoda, Y., and Yanagida, M. (2004). A conserved Mis12 centromere complex is linked to heterochromatic HP1 and outer kinetochore protein Zwint-1. Nat. Cell Biol. *6*, 1135–1141.

Okada, M., Cheeseman, I.M., Hori, T., Okawa, K., McLeod, I.X., Yates, J.R., Desai, A., and Fukagawa, T. (2006). The CENP-H-I complex is required for the efficient incorporation of newly synthesized CENP-A into centromeres. Nat. Cell Biol. *8*, 446–457.

Ong, S.E., Blagoev, B., Kratchmarova, I., Kristensen, D.B., Steen, H., Pandey, A., and Mann, M. (2002). Stable isotope labeling by amino acids in cell culture, SILAC, as a simple and accurate approach to expression proteomics. Mol. Cell. Proteomics *1*, 376–386.

Porter, I.M., McClelland, S.E., Khoudoli, G.A., Hunter, C.J., Andersen, J.S., McAinsh, A.D., Blow, J.J., and Swedlow, J.R. (2007). Bod1, a novel kinetochore protein required for chromosome biorientation. J. Cell Biol. *179*, 187–197.

Raaijmakers, J.A., Tanenbaum, M.E., Maia, A.F., and Medema, R.H. (2009). RAMA1 is a novel kinetochore protein involved in kinetochore-microtubule attachment. J. Cell Sci. *122*, 2436–2445.

Rappsilber, J., Ishihama, Y., and Mann, M. (2003). Stop and go extraction tips for matrix-assisted laser desorption/ionization, nanoelectrospray, and LC/MS sample pretreatment in proteomics. Anal. Chem. *75*, 663–670.

Rappsilber, J., Ryder, U., Lamond, A.I., and Mann, M. (2002). Large-scale proteomic analysis of the human spliceosome. Genome Res. *12*, 1231–1245.

Schirmer, E.C., Florens, L., Guan, T., Yates, J.R., 3rd, and Gerace, L. (2003). Nuclear membrane proteins with potential disease links found by subtractive proteomics. Science *301*, 1380–1382.

Shevchenko, A., Tomas, H., Havlis, J., Olsen, J.V., and Mann, M. (2006). In-gel digestion for mass spectrometric characterization of proteins and proteomes. Nat. Protoc. *1*, 2856–2860.

Takata, H., Uchiyama, S., Nakamura, N., Nakashima, S., Kobayashi, S., Sone, T., Kimura, S., Lahmers, S., Granzier, H., Labeit, S., et al. (2007). A comparative proteome analysis of human metaphase chromosomes isolated from two different cell lines reveals a set of conserved chromosome-associated proteins. Genes Cells *12*, 269–284.

Theis, M., Slabicki, M., Junqueira, M., Paszkowski-Rogacz, M., Sontheimer, J., Kittler, R., Heninger, A.K., Glatter, T., Kruusmaa, K., Poser, I., et al. (2009). Comparative profiling identifies C13orf3 as a component of the Ska complex required for mammalian cell division. EMBO J. *28*, 1453–1465.

Tkaczuk, K.L., Dunin-Horkawicz, S., Purta, E., and Bujnicki, J.M. (2007). Structural and evolutionary bioinformatics of the SPOUT superfamily of methyltransferases. BMC Bioinformatics *8*, 73.

Uchiyama, S., Kobayashi, S., Takata, H., Ishihara, T., Hori, N., Higashi, T., Hayashihara, K., Sone, T., Higo, D., Nirasawa, T., et al. (2005). Proteome analysis of human metaphase chromosomes. J. Biol. Chem. *280*, 16994–17004.

Van Hooser, A.A., Yuh, P., and Heald, R. (2005). The perichromosomal layer. Chromosoma *114*, 377–388.

Welburn, J.P., Grishchuk, E.L., Backer, C.B., Wilson-Kubalek, E.M., Yates, J.R., 3rd, and Cheeseman, I.M. (2009). The human kinetochore Ska1 complex facilitates microtubule depolymerization-coupled motility. Dev. Cell *16*, 374–385.

Wen, H., Li, J., Song, T., Lu, M., Kan, P.Y., Lee, M.G., Sha, B., and Shi, X. (2010). Recognition of histone H3K4 trimethylation by the plant homeodomain of PHF2 modulates histone demethylation. J. Biol. Chem. *285*, 9322–9326.

Wu, W.H., Alami, S., Luk, E., Wu, C.H., Sen, S., Mizuguchi, G., Wei, D., and Wu, C. (2005). Swc2 is a widely conserved H2AZ-binding module essential for ATP-dependent histone exchange. Nat. Struct. Mol. Biol. *12*, 1064–1071.